

Erosive Corrosive Wear Performance of Single Layer CrN Coatings on AISI 304 Stainless Steel in Sea Water Centrifugal Pumps using Steady State Analysis

Alok Vats

M. Tech, Production Engineering, MNIT Jaipur, Pass out 2016

Address: Plot No. 761 Mundka, New Delhi- 110041 (Near Swati Modern Public School)

Abstract— The purpose of present study was to investigate the erosive corrosive wear behavior of single layer (CrN) coatings on AISI 304 Stainless Steel samples with varying coating thickness (0-200 nm) in the range of 50 nm. The slurry jet erosive test was conducted on Slurry Jet Erosion Tester in saline slurry (3.5wt% salt) under the different working conditions with varying impact velocity (10-25 m/s), impingement angle (30°-75°) and erodent discharge (160-280 gm/min). Steady state analysis was applied to find optimum parameters for the minimization of erosion rate of various coated and uncoated samples. The finding of steady state condition tests indicated that the erosion rate increased with the increase in impact velocity and erodent discharge but decreased with the increase in coating thickness. The results also indicated that erodent discharge was the most significant factor, followed by impingement angle and impact velocity for the CrN coated samples. The SEM characterization of the eroded samples was carried out in order to analyze the topography of the eroded surface to investigate the wear mechanisms induced by slurry jet erosion test.

Keywords— Erosive wear, corrosive wear, single layer coating, Steady state analysis, Scanning electron microscope (SEM).

I. INTRODUCTION

Erosion-corrosion is the increase in the rate of degradation of the material caused by the combined action of electrochemical corrosion and mechanical wear processes. Corrosion is a material degradation process which occurs due to electrochemical action, while erosion is a mechanical wear process. When these two processes act together especially in the marine environments, it is known as erosion-corrosion. It is one of the major causes of failure in the nuclear power plants, chemical, petrochemical industries and marine environments where combined effect of erosion and corrosion phenomena occurs. In the marine field, this study applies to ship and boats. The study is

equally beneficial in those areas where the underground salty water is supplied for household purposes, and the same has to be delivered to the overhead tank.

In the liquid-particle flow, the sand particles get impinged on steel surface which remove a layer of protective film from its surface. The chloride ions act rapidly on the exposed surface having discontinuity. In this way pure erosion and erosion enhanced corrosion are the dominant mechanisms that degrade the metal surface in erosion corrosion [1-6]. In order to improve the physical, mechanical and surface wear of metal such as steel, surface treatment such as modification of surface using silane, electroplating, Nitriding and coating etc are used [7-13]. A majority of surface modification lead to improved corrosive characteristics of the steel. Hence, they are also called corrosion inhibitors and are used on variety of steels. Neville et al. [7] studied erosion-corrosion of engineering steels by the use of chemicals on X65 pipeline steel, 13Cr martensitic stainless steel and super-duplex stainless steels. They concluded that inhibitor has a greater effect on the corrosion component of carbon steel but offers no protection on super-duplex stainless steel under the conditions tested. In another research, Hu et al. [14] assessed the effect of corrosion inhibitor on erosion-corrosion of API-5L-X65 stainless steel in multi-phase jet impingement conditions and found that corrosion inhibitor provides up to 20% protection in erosion-corrosion conditions and that oil phase reduces the erosion component by reducing the particle velocity in the flow conditions. Yao et al. [15] investigated a new method for protecting bends from erosion in gas-particle flows and reported that adding ribs on the outer-wall of the inside bend can significantly improve bend's erosion protection ability. Surface coating technology has also been deployed to enhance the erosive corrosive characteristics of the metals. Multilayer coatings offer protection against synergistic effects on bare stainless steel surfaces.

Corrosion resistance can also be increased by providing an interlayer of a suitable material [16]. Coatings of CrN and CrCN have been commonly used in industry and research to improve surface properties of materials. However, CrCN coatings provide better corrosion resistance than CrN coated samples due to its superior mechanical properties [17]. Shan et al. [18] fabricated CrN coatings on 316L stainless steel substrate by multi-arc ion plating system, performed Polarization tests and concluded that the multilayer structure could limit the crack propagation only to the layer and reduce cracks in the coating. However, there are various other factors besides the coating thickness that affect the erosive corrosive performance under practical conditions. These are impact velocity, impingement angle and erodent discharge respectively. The erosive corrosive performance of the material under a given combination of these factors has not been fully understood.

Hence, the aim of this work was to fabricate single layer coated AISI 304 stainless steel material, study the effect of various parameter such as coating thickness, impact velocity, erodent discharge and impingement angle on the erosive and corrosive behavior of fabricated material and finally to find different levels of factors to achieve a condition of minimum wear rate using steady state approach.

II. EXPERIMENTAL PROCEDURE

2.1 Materials

The proposed work consists of deposition of mono-layered PVD coatings of CrN of varying thickness on AISI 304 stainless steel. AISI 304 stainless steel was purchased from Bahubali Steels, New Delhi. While Chromium powder was procured from M/s Indian Diamond Tools and M/s Scientific Instruments, Jaipur, India. The detailed properties and specification of the selected materials are presented in the Table 1.

2.2 Sample Preparation and Coating Process

The samples for coating were prepared as per test standard specification with the help of a diamond cutter. Then the uncoated samples were mirror-polished using a MetaServe 250 Grinder Polisher (Buhler machine, Illinois, USA). The fine polish provides the improvement of adherence between coating and the samples. Before coating, samples were cleaned in acetone and then dried in a pre-vacuum dryer. The pellets used for coating were prepared with the help of 99.5% pure Cr powder procured from M/s Indian Diamond Tools and M/s Scientific Instruments, Jaipur. The pellet were pressed using a KBr press at a pressure of 15 tonnes.

A thermal Vapor deposition process (inside a high temperature Vacuum Box Coater -Model BC-300, Hind

High Vacuum Co. (P) Ltd. Bangalore, India) (Figure.1) was used to fabricate single layer (chromium nitride) coated AISI 304 Stainless Steel with varying coatings thickness (50nm, 100nm, 150nm and 200nm). In this coating process, a sample of AISI 304 Stainless Steel was first positioned in the sample holder. Then a tungsten filament was used to hold the pellet of pure chromium. A high vacuum of 10^{-3} bar was created inside the chamber and current (50-75 A, 12 V) was supplied to the tungsten filament to evaporate pure chromium. Then, nitrogen gas was allowed to flow in the chamber which reacted with the evaporated chromium and a layer of chromium nitride was deposited on the surface of the AISI 304 Stainless Steel. Coating thickness was maintained as 50nm, 100nm, 150nm and 200nm. Parameters for CrN coating were taken as coating rate- 0.1 Å/sec, coating thickness-200nm, Vacuum Chamber temperature-2000°C, Vacuum Pressure- 1.2×10^{-6} bar, Nitrogen flow rate- 50cc/min, Voltage-12V, Current-39 Ampere.

2.3 Sample characterization

2.3.1 Slurry Jet Erosion Test

The slurry erosion behavior of single layer CrN coated and uncoated samples was evaluated using a Slurry Jet Erosion Tester (Model TR411, Ducom, India) (Figure. 2). For this test, slurry was prepared by mixing sand particles and water and taken in the hopper. Square samples of dimensions 25×25 mm was placed in the sample holder. Samples were eroded by flow of erodent discharge through a nozzle of 4 mm diameter. Impingement angles were changed by adjusting the sample holder at different angles (30° , 45° , 60° and 75°). The strike was applied for 10 min. The weight loss was determined by the weighing the sample before and after the slurry erosion test. The slurry erosion rate was calculated by dividing weight loss of samples with the time taken to perform an experiment i.e. 10min.

2.3.2 Field Emission Scanning electron microscope (FE-SEM)

The eroded surfaces of the samples were examined under SEM to find out the effect of varying each of parameters in the wear behavior of coated and uncoated materials. The SEM characterization was carried out by using a FEI NOVA NANOSEM 450 to investigate the wear mechanisms induced by slurry jet erosion test.

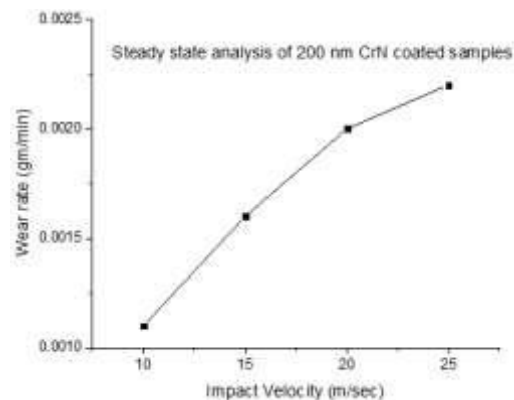
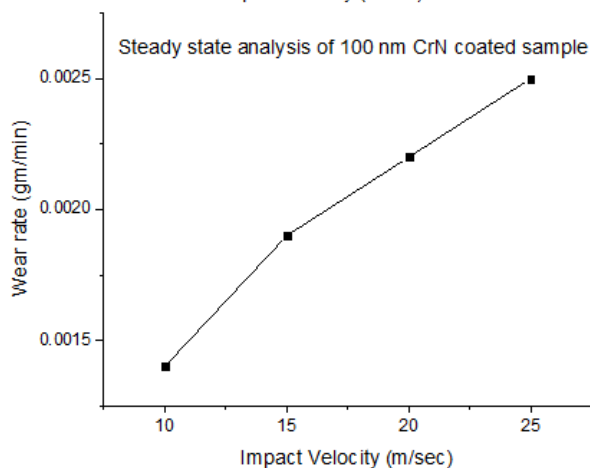
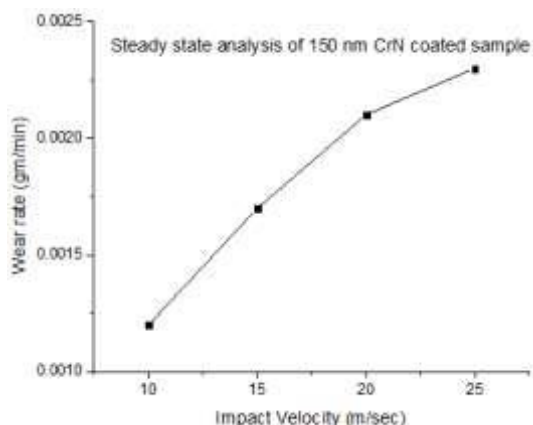
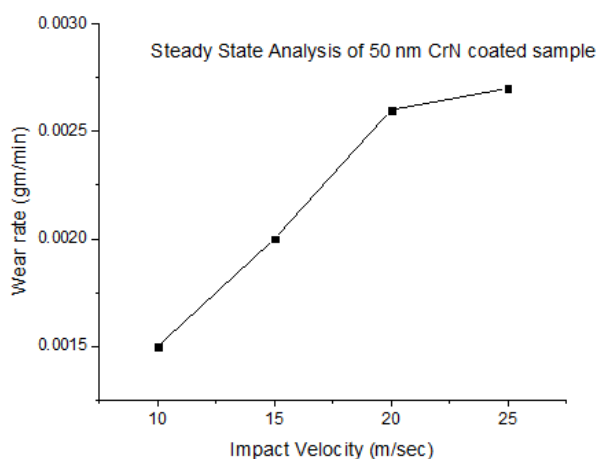
III. RESULTS AND DISCUSSION

3.1 Wear Characteristic analysis using Steady State condition

3.1.1 Effect of varying impact velocity on the wear characteristic of CrN coated and uncoated AISI 304 Stainless Steel samples of different coating thickness

In this steady state analysis impact velocity was varied in the range of (10-25m/sec) to study their effect on slurry erosion rate of uncoated and single layer CrN coated AISI 304 stainless steel with coating thicknesses (50nm, 100nm, 150nm and 200nm) while keeping all others parameters constant such as (impingement angle 45°, erodent discharge 160 gm/min and time 10 minute). Figure 3 indicated the wear rate of uncoated and single layer coated AISI 304 stainless steel with different thickness at different impact velocities (10-25 m/s). Figure 3 also indicated that the slurry erosion rate increased with the increase in impact velocity for all coated materials. But for a particular coating thickness, this increment goes on diminishing as impact velocity is increased. The decrease in wear rate with the increase in coating thickness was attributed to the increase in hardness of the coating along with an increase in its thickness due to which there was less penetration of the erodent particles into the coating or the base metal. Another reason for such behaviour was work hardening of either the coating or the base metal.

Both the hardness and work hardening capability of the coating depend on the sample preparation process (grinding of samples, polishing, effective cleaning etc.) and coating conditions like magnitude of vacuum developed and temperature. It was further revealed from Figure 3 that the increase in coating thickness led to decrease in wear rate. An observation similar to this for steady state analysis was made by Patnaik et al. [19] while working on chromium nitride coated aluminum alloys which were reinforced by varying percentage of granite. Rajahrama et al. performed erosive corrosive test on stainless steel (SS316L), Carbon steel (AISI 1020) and nickel-aluminium-bronze (NAB) and found that increasing the velocity and sand concentration produced higher mass loss rates [20]. Yao et al. [21] have worked on 316 and 304 grades of Austenitic stainless steels in Flow Jet Impingement apparatus. They have reported that mass loss per unit area in both the steels followed a linear relationship with time.



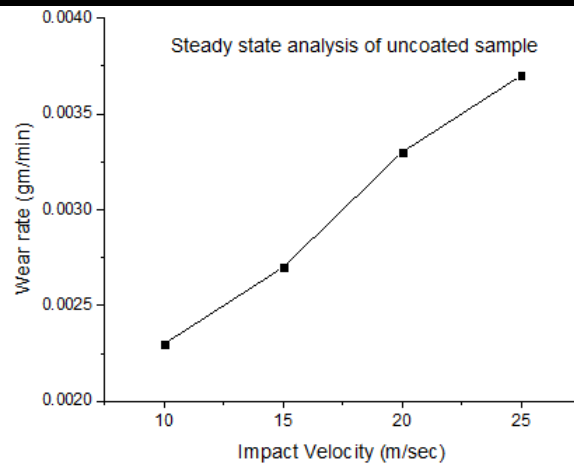


Fig.3: Effect of varying Impact velocity on the wear rate on single layer (CrN) coated and uncoated AISI 304 Stainless Steel



Fig.2: Test setup of Slurry Jet Erosion Tester



Fig.1: Thermal/E-beam PVD Coating Unit

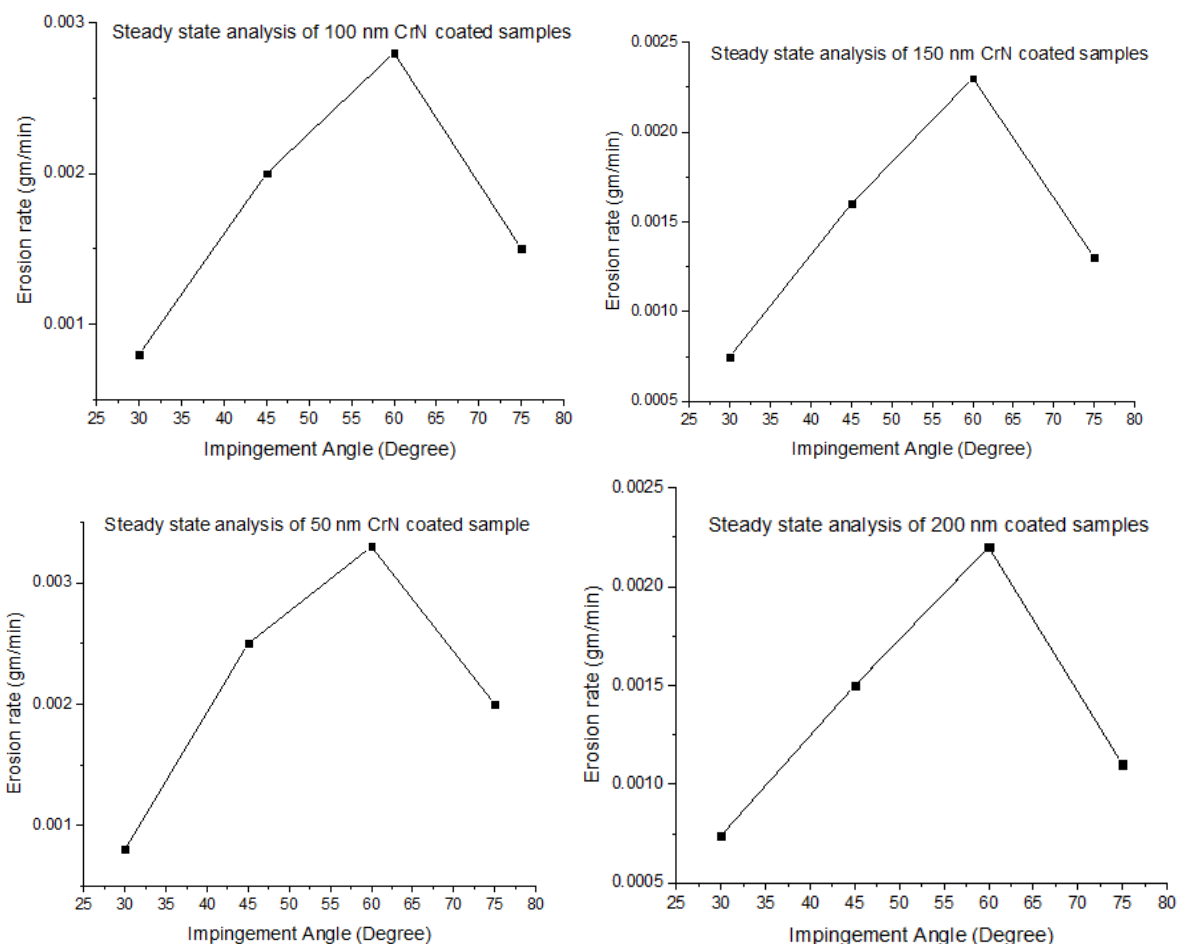
3.1.2 Effect of varying impingement angle on the wear characteristic of CrN coated and uncoated AISI 304 Stainless Steel samples of different coating thickness

Figure 5 show the erosion rate of CrN coated and uncoated AISI 304 Stainless Steel samples in slurry jet environment for different impingement angle keeping all other parameters constant (impact velocity 15m/sec, erodent discharge 160 gm/min and time 10 minute). It has been already reported that jet erosive wear was greatly affected by the working conditions [22]. From Figure 4, it can be seen that erosion rate was increased when the impingement angle was increased from 30° to 60° but later in the range 60° to 75° it was decreased. Hence, it can be concluded that the erosive wear was maximum at 60° impingement angle. It was attributed to the facts that at 60° impingement angles both erosion and abrasion worked simultaneously on the samples. During the test, the sand particles eroded first and again slide over on the surface

while dropping down. Thus the materials were removed due to impact energy (erosion) as well as sliding energy (abrasion). On the other hand, at 30° impingement angle, the material were removed due to sliding (abrasion) only, at 75° impingement angle material were removed due to impact energy (erosion) only and at 45° impingement angle material were removed due to partial effect of both the erosion and abrasion. Finally both the effect became predominant at 60° impingement angle.

Further it was revealed from Figure 4 that the rate of increase of erosion rate decreased as the angle increased from 30° to 60° due to work hardening of either the coating or the base metal.

Work hardening is a function of impact energy which goes on increasing as the impingement angle increases. Greater the impact energy at higher angles, greater is the work hardening and less is the increase in erosion rate.



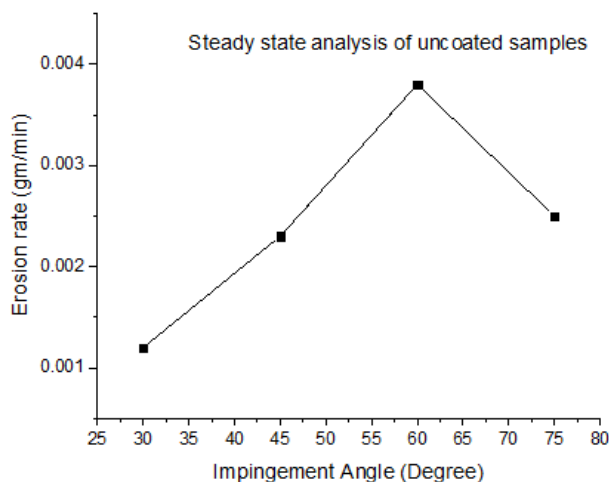


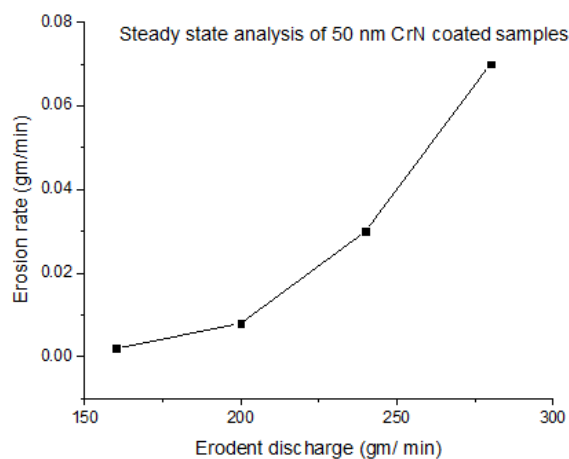
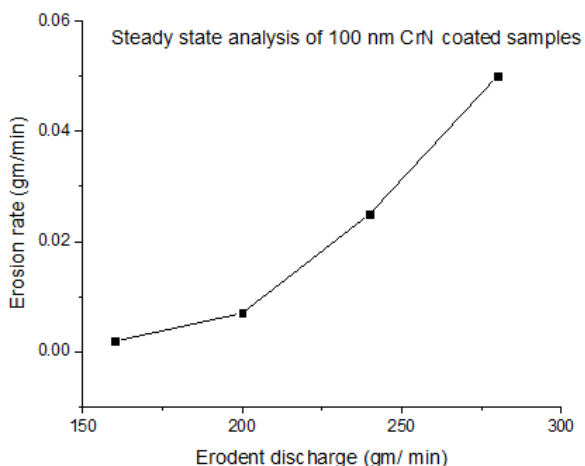
Fig.4: Effect of varying impingement angles on the wear rate on single layer (CrN) coated and uncoated AISI 304 Stainless Steel

3.1.3 Effect of varying erodent discharge on the wear characteristic of CrN coated and uncoated AISI 304 Stainless Steel samples of different coating thickness

Figure 5 show the erosion rate of CrN coated and uncoated AISI 304 Stainless Steel samples in slurry jet environment for different erodent discharge from 160 gm/min to 280 gm/min keeping all other parameters constant (impact velocity 15m/sec, impingement angle 45° and time 10 minute). From Figure 5, it can be seen that erosion rate was increased with the increase in erodent discharge. Increase in erosion rate with the increase in erodent discharge was attributed to the fact that more abrasive particle participated in the erosive and abrasive wear. Hence, more materials were removed. Further it was also revealed that there was more wear in uncoated sample as compared to coated sample. In this regard, it was observed the erosion rate of uncoated sample at 280 gm/min of erodent discharge was 47.05% more than the erosion rate of single layer (CrN) coated AISI 304 Stainless Steel with coating thickness 50nm. Further it was revealed from Figure 5 that the rate of

increase of erosion rate increases with increase in the erodent discharge. Here, the effect of work hardening is overcome by more number of erodent particles striking the samples per unit time. Out of all the three steady state experiments the greatest material is removed when erodent discharge is increased. It is because in erosion wear, every particle with a certain velocity imparts some force which removes the material from the sample. Greater the number of particles, greater is the magnitude of force which removes the material and causes wear. The next higher material is removed when impingement angle is varied, while the least material is removed when velocity is varied in the steady state experiments keeping all other parameters constant.

These results indicate that for the CrN coated samples with varying coating thickness (0-200 nm) in the range of 50 nm, erodent discharge is the most significant factor, followed by impingement angle and impact velocity. It means that impact velocity is the least significant factor in case of CrN coated steels.



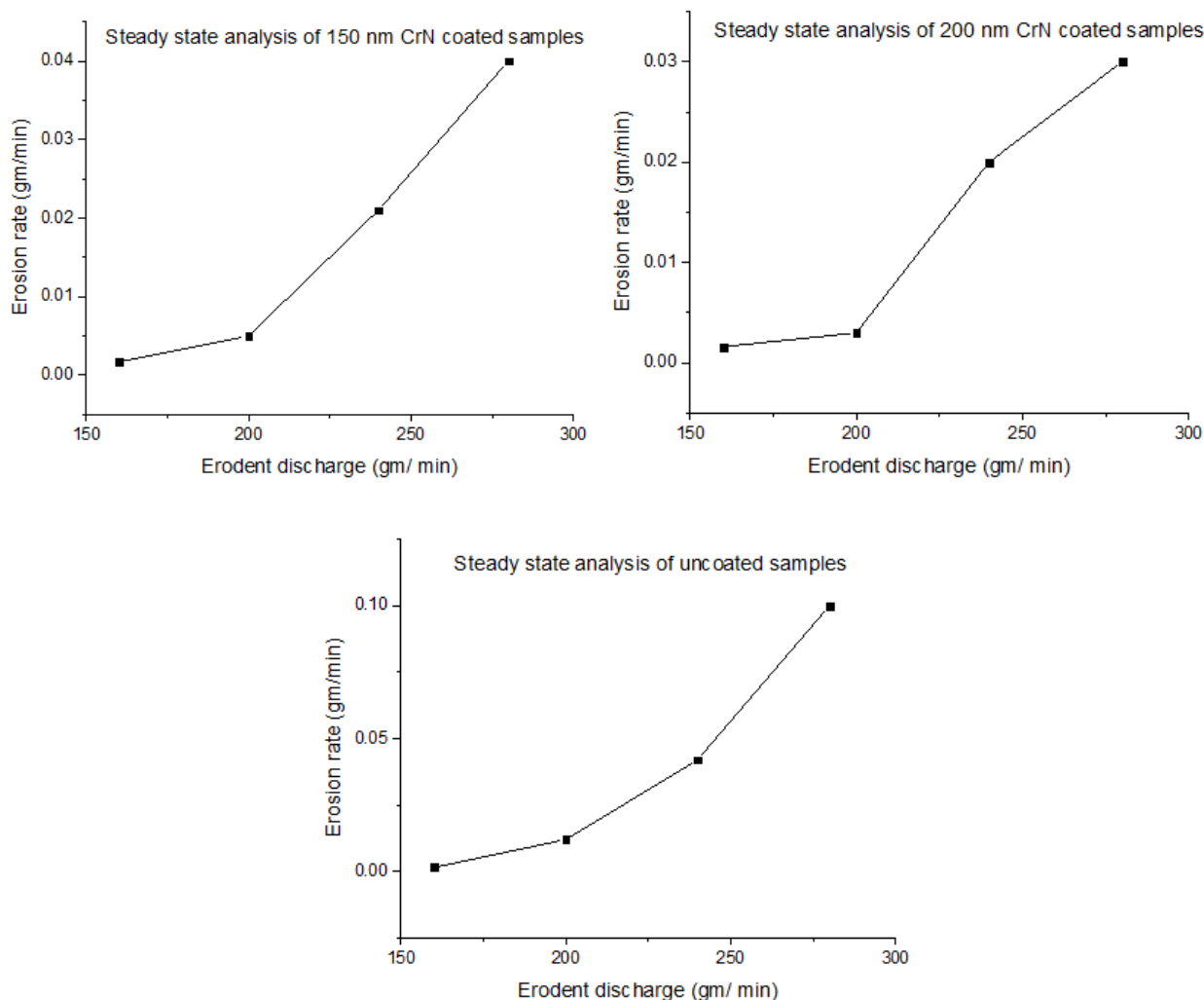


Fig.5: Effect of varying erodent discharge on the wear rate on single layer (CrN) coated and uncoated AISI 304 Stainless Steel

3.2 Surface Morphology of Worn coated and uncoated Samples

Figure 6 (a-g) represented the surface morphology of worn surface of coated and uncoated AISI-304 Steel. From the SEM images (a-d) it can be observed that as the impact velocity was increased the mode of erosion wear changed from small holes and grooves to lip formation and deep craters. This led to an extensive deformation at large velocities and hence an increase in mass loss or erosion rate for a particular coating thickness. However, as the impact velocity increased, an increase in the rate of work hardening took place. It was due to the repeated number of impacts which work hardened the coating as well as the base metal, in case the coating was wiped off from certain areas of the sample. From Table 2 it was evident that the erosion rate increased with increase in impact velocity under steady state conditions. The exception was sample 4 in which erosion rate was less than sample 3. This may be

due to high coating thickness or antagonistic synergy during erosive corrosive wear.

In uncoated 304 steel samples with increase in impact velocity mass loss decreased due to increase in impingement angle. At large angles, normal force increased indentation like marks form on the surface. These indentation marks were due to embedding of the sand particles which in turn increase the rate of work hardening. Therefore, less wear was obtained at larger angles that can be seen from Figure 6 (f) and Table 2 (condition 6). Also a high erodent discharge as evident in Table 2 (condition 6), leads to work hardening only if particles get embedded into the samples. Also, cracks were formed due to the movement of the sand particles into the subsurface which has created a highly stressed region [23]. This in turn, leads to the development of large cracks and more work hardening.

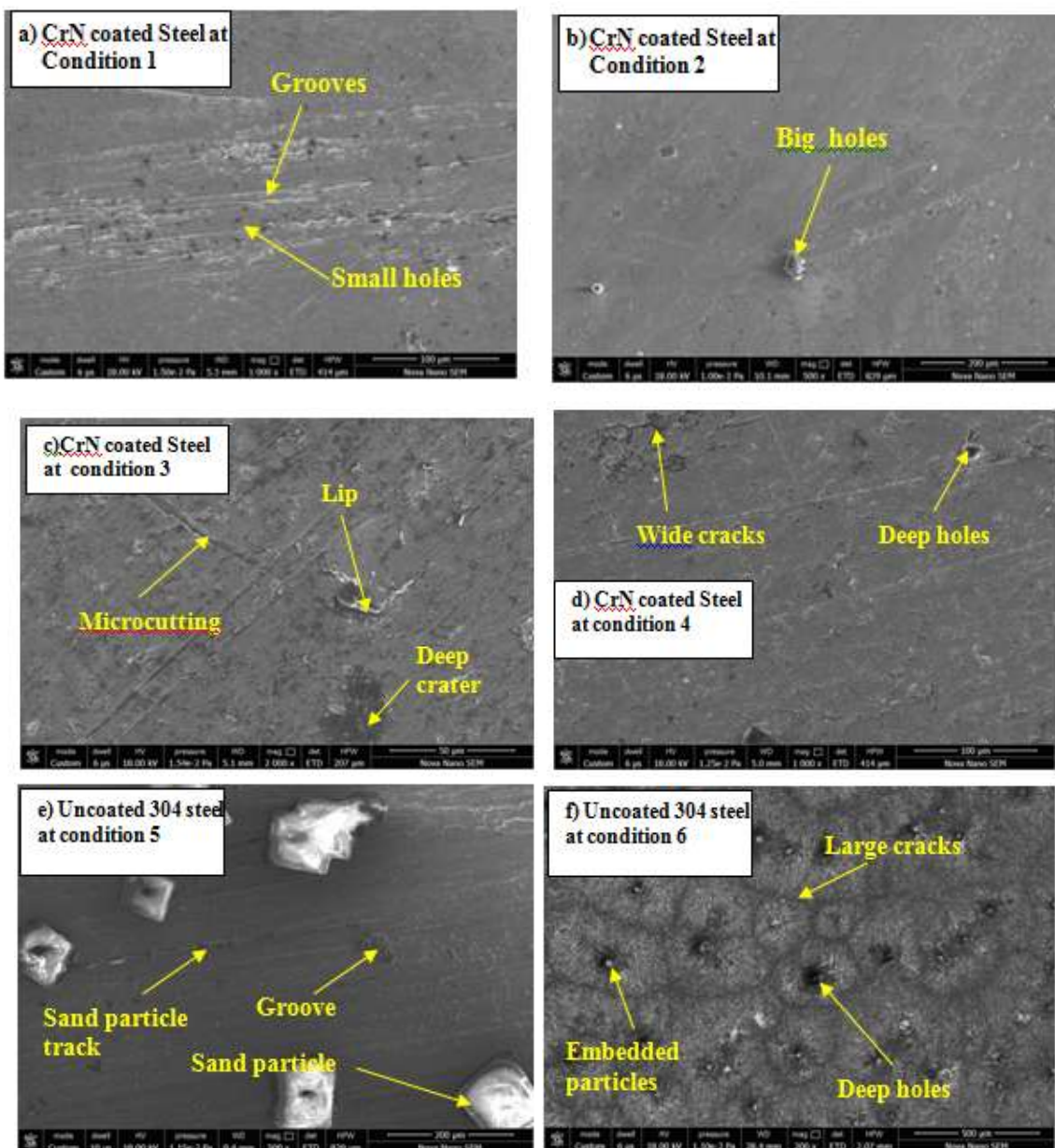
Groove formation is a function of sliding velocity (abrasion). Greater it is, larger is the movement of sand

particles along the surface and larger is the size of the groove. Since sliding energy is the main energy for material removal at smaller angles, it means that grooves are the main cause of wear when impingement angles are small (30°). Similar results were obtained by Wood et al. [24] who worked on 316 steels and concluded that both erosion and erosion– corrosion surfaces exhibited similar surface features like impact crater, particle embedment and crater lip formation. However, at smaller angles Grooves formation and sand particle tracks were main modes of erosive wear. At higher angles the decrease in sliding energy leads to lesser movement of the sand particles along the sample surface. However an increase in impact energy at higher angles creates deeper indentation

into the coating. Both these lead to the formation of deep grooves. It is evident from Figure 6 (c-d).

Small holes and big holes are points of discontinuities developed due to corrosive action of the medium. From Table 2 it is seen that holes are formed at low velocities (condition 1 and 2). It is due to the fact that at low velocities chloride ions in water get more time to act upon and enhance corrosion. Such a situation gives rise to corrosion enhanced erosion. It means that at low velocities corrosion enhanced erosion is more dominant.

Lip formation requires both impact as well as sliding energy. Since at angles of around 45° material removal takes place partly by means of sliding and partly by means of impact energy, lip formation is also observed to appear at 45° and is evident from Figure 6 (c-d).



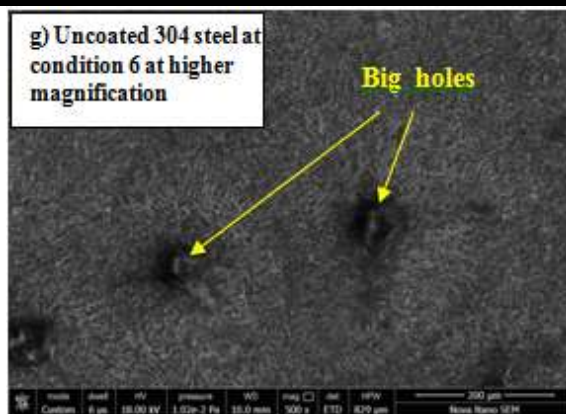


Fig.6: FE-SEM images of CrN coated and Uncoated SS-304 steel specimens after erosive wear

Table.2: Various erosion conditions of worn out samples for SEM and their erosion rate

Sample No. Condition No.	Coating thickness (nm)	Impact velocity (m/sec)	Impingement angle (degrees)	Erodent discharge (gm/min)	Dominant wear mechanism	Erosion rate or mass loss
1	50	10	45	160	Grooves formation, small holes	0.0015
2	100	15	45	160	Big holes	0.0016
3	150	20	45	160	Lip formation, deep grooves	0.0021
4	200	25	45	160	Lip formation, deep grooves	0.0020
5	Uncoated 304 steel samples	20	30	160	Grooves formation	0.0028
6		25	75	240	Large cracks, embedded particles, deep holes	0.0025

Table.1: Properties of AISI 304 stainless steel

S. No	Property	Specifications
1.	Density	8g/cc
2.	Rockwell Hardness B	70
3.	Tensile Strength, Ultimate	505 Mpa
4.	Tensile Strength, Yield	215 Mpa
5.	Elongation at Break point	70 %
6.	Modulus of Elasticity	195- 200 Gpa
7.	Charpy Impact	325 J
8.	Shear Modulus	86 Gpa
9.	CTE, linear 20°C	17.3 µm/m-°C
10.	CTE, linear 250°C	17.8 µm/m-°C
11.	CTE, linear 500°C	18.7 µm/m-°C
12.	Specific Heat Capacity	0.5 J/g-°C
13.	Thermal Conductivity at Elevated Temperature	16.2 W/m-K
14.	Melting Point	1400- 1455 °C

IV. CONCLUSIONS

1. For the steady state analysis with variation in impingement velocity for the CrN coated samples with varying coating thickness (0-200 nm) in the range of 50 nm, the erosion rate increased with increase in impact velocity. But the rate of increase of erosion rate decreased as the coating thickness increased. It could be due to increase in hardness or work hardening of coating as the coating thickness increased. It concludes that the coating deposition enhanced the wear performance.
2. Both the hardness and work hardening capability of the coating depend on the sample preparation process (grinding of samples, polishing, effective cleaning etc.) and coating conditions like magnitude of vacuum developed and temperature.
3. For the steady state analysis with variation in impact angle, the erosion rate increased from 30° to 60° but later in the range 60° to 75° it was decreased. Hence, it can be concluded that the erosive wear was maximum at 60° impingement angle. It was attributed to the fact that at 60° impingement angles both erosion and abrasion worked simultaneously on the samples.
4. Work hardening, for the steady state analysis with variation in impact angle, is a function of impact energy which goes on increasing as the impingement angle increases. Greater the impact energy at higher angles, greater is the work hardening and less is the increase in erosion rate.
5. For the steady state analysis with variation in erodent discharge, the effect of work hardening was overcome by more number of erodent particles striking the samples per unit time. Out of all the three steady state experiments the greatest material is removed when erodent discharge is increased.
6. For the CrN coated samples with varying coating thickness (0-200 nm) in the range of 50 nm, erodent discharge is the most significant factor, followed by impingement angle and impact velocity. It means that impact velocity is the least significant factor in case of CrN coated steels.
7. Groove formation is a function of sliding velocity (abrasion). Greater it is, larger is the movement of sand particles along the surface and larger is the size of the groove. Since sliding energy is the main energy for material removal at smaller angles, it means that grooves are the main cause of wear when impingement angles are small (30°).
8. At higher angles the decrease in sliding energy leads to lesser movement of the sand particles along the sample surface. However an increase in

impact energy at higher angles creates deeper indentation into the coating. Both these lead to the formation of deep grooves.

9. Small holes and big holes are points of discontinuities developed due to corrosive action of the medium. It is due to the fact that at low velocities chloride ions in water get more time to act upon and enhance corrosion. Such a situation gives rise to corrosion enhanced erosion. It means that at low velocities corrosion enhanced erosion is more dominant.
10. Lip formation requires both impact as well as sliding energy. Since at angles of around 45° material removal takes place partly by means of sliding and partly by means of impact energy, lip formation is also observed to appear at 45°.
11. SEM analysis of the samples eroded at steady state shows a transition of the wear mechanism from grooves and small holes to big holes and craters. In some samples large cracks were also seen. At high velocities sand particles get embedded in the samples. These embedded particles work hardened the base material and therefore reduction in the erosion rate of base steel was observed.

REFERENCES

- [1] Zhang, G. A., Xu, L. Y., Cheng, Y. F. (2009) Investigation of erosion–corrosion of 3003 aluminum alloy in ethylene glycol–water solution by impingement jet system, *Corros. Sci.* 51, pp 283–290.
- [2] Shrestha, S., Hodgkiess, T., Neville, A. (2005) Erosion-corrosion behavior of high-velocity oxy-fuel Ni–Cr–Mo–Si–B coatings under high-velocity seawater jet impingement, *Wear* 259, pp 208–218
- [3] Saha, G. C., Khan, T. I. G. A. Zhang, (2011), Erosion–corrosion resistance of microcrystalline and near-nanocrystalline WC–17Co high velocity oxy-fuel thermal spray coatings, *Corros. Sci.* 53, pp 2106–2114.
- [4] Hong, S., Wu, Y., Zhang, J., Zheng, Y., Qin, Y., Lin, J. (2015), Effect of ultrasonic cavitation erosion on corrosion behavior of high-velocity oxygen-fuel (HVOF) sprayed near-nanostructured WC-10Co-4Cr coating, *Ultrason. Sonochem.* 27, pp 374–378.
- [5] Zhao, Y., Zhou, F., Yao, J., Dong, S., Li, N., (2015), Erosion–corrosion behaviour and corrosion resistance of AISI 316 stainless steel in flow jet impingement, *Wear* 328-329, pp 464–474.
- [6] Lin, C. K., Hsu, C. H., Cheng, Y. H., Liang, O. K., Lee, S. L. (2015), A study on the corrosion and

- erosion behavior of electroless nickel and TiAlN/ZrN duplex coatings on ductile iron, *Appl. Surf. Sci.* 324, pp 13–19.
- [7] Neville, A., Wang, C. (2009), Erosion–corrosion of engineering steels—Can it be managed by use of chemicals, *Wear* 267, pp 2018–2026.
- [8] Pantoja, M., Abenojar, J., Martínez, M. A., Velasco, F. (2016), Silane pretreatment of electrogalvanized steels: Effect on adhesive properties, *International Journal of Adhesion and Adhesives* 65, pp 54-62.
- [9] Pantoja, M., Martínez, M. A., Abenojar, J., Encinas, N., Ballesteros, Y. (2011), Effect of EtOH/H₂O ratio and pH on bis-sulfur silane solutions for electrogalvanized steel joints based on anaerobic adhesives, *The Journal of Adhesion* 87 (7-8), pp 688-708.
- [10] Martínez, M. A., Calabrés, R., Abenojar, J., Velasco, F., (2008), Sintered High Carbon Steels: Effect of Thermomechanical Treatments on their Mechanical and Wear Performance, *Materials Science Forum* 591, pp 271-276.
- [11] Pantoja, M., Martínez, M. A., Abenojar, J., Velasco, F., Real, J. C. (2010), Structural and mechanical characterization of γ -methacryloxypropyltrimethoxysilane (MPS) on Zn-electrocoated steel *Journal of Adhesion Science and Technology* 24 (11-12), pp 1885-1901.
- [12] Pantoja, M., Velasco, F., Broekema, D., Abenojar, J., Real, J. C. (2011), The influence of pH on the hydrolysis process of γ -methacryloxypropyltrimethoxysilane, analyzed by FT-IR, and the silanization of electrogalvanized steel, *Journal of Adhesion Science and Technology* 24(6), pp 1131-1143.
- [13] Recco, A. A., Lopez, C. D., Bevilacqua, A. F., da Silva, F., Tschiptschin, A. P. (2007),
- [14] Improvement of the slurry erosion resistance of an austenitic stainless steel with combinations of surface treatments: Nitriding and TiN coating, *Surf. Coat. Tech.* 202, pp 993–997.
- [15] Hu, X., Alzawai, K., Gnanavelu, A., Neville, A., Wang, C., Crossland, A., Martin, J. (2011), Assessing the effect of corrosion inhibitor on erosion–corrosion of API-5L-X65 in multi-phase jet impingement conditions, *Wear* 271, pp 1432–1437.
- [16] Yao, J., Zhang, B. Z., Fan, J. R. (2000), Investigation of a new protection method for protecting tube from erosion in gas-particle flows, *J. Therm. Sci.* 9(2), pp 158-162.
- [17] Wood, R. J. K. (2007) Tribo-corrosion of coatings: a review, *J. Phys. D. Appl. Phys.* 40(18), pp 5502-5521.
- [18] Ye, Y., Wang, Y., Chen, H., Li, J., Yao, Y. (2015) Doping carbon to improve the tribological performance of CrN coatings in seawater, *Tribol. Int.* 90, pp 362–371.
- [19] Shan, L., Wang, Y., Li, J., Jiang, X., Chen, J. (2015) Improving tribological performance of CrN coatings in seawater by structure design, *Tribol. Int.* 8278–88.
- [20] Gautam, V., Patnaik, A., Bhat, I. K. (2016) Microstructure and Wear Behavior of Single layer (CrN) and Multilayered (SiN/CrN) Coatings on Particulate Filled Aluminum Alloy Composites, *Silicon* DOI 10.1007/s12633-015-9357-9.
- [21] Rajahram, S. S., Harvey, T. J., Wood, R. J. K. (2009) Erosion–corrosion resistance of engineering materials in various test conditions, *Wear* 267, pp 244–254.
- [22] Yao, J., Zhou, F., Zhao, Y., Yin, H., Guo, Q., Li, N. (2015) Experimental Investigation of Erosion of Stainless Steel by Liquid-solid Flow Jet Impingement, *Procedia Eng.* 102, pp 1083 – 1091.
- [23] Hutchings, I. (1992) Ductile–brittle transitions and wear maps for the erosion and abrasion of brittle materials. *J. Phys D Appl. Phys.* 25, pp A212–A221.
- [24] Rajahram, S. S., Harvey, T. J., Walker, J. C., Wang, S. C., Wood, R. J. K. (2012) Investigation of erosion–corrosion mechanisms of UNS S31603 using FIB and TEM, *Tribol. Int.* 46, pp 161–173.
- [25] Wood, R. J. K., Walker, J. C., Harvey, T. J., Wang, S., Rajahram, S. S. (2013) Influence of microstructure on the erosion and erosion–corrosion characteristics of 316 stainless steel, *Wear.* 306, pp 254–262.